ICANS-XVII
17th Meeting of the International Collaboration on Advanced Neutron Sources
April 25-29, 2005
Santa Fe, New Mexico

Phase II Solid Methane Scattering Kernel with Comparison to LENS Energy Spectrum Measurement

Y. Shin[1], W. M. Snow[1], C. M. Lavelle[1], D. V. Baxter[1], M. B. Leuschner[1], W. Lozowski[1], H. Nann[1], N. Remmes[1], T. Rinckel[1], and P. E. Sokol[1]

[1] Department of Physics, Indiana University/IUCF, 2401 Milo B. Sampson Lane, Bloomington, IN 47408, USA

Abstract

Methane is one of the few substances that possess free rotor groups even in the solid phase at low temperature. These rotational degrees of freedom allow for efficient energy loss for cold neutrons and CH4 is therefore a good choice for a low energy neutron moderator. . In addition to its use as a cold neutron moderator at LENS, solid methane is planned to be used as a pre moderator for an ultracold neutron (UCN) source at the NC State PULSAR reactor and can also be used as a premoderator for a SO2 UCN source at LENS. We have developed a model for the double differential cross section for solid methane for incident neutron energies E_i from 0.1 meV to 165 meV and temperatures from 4 K to 20 K. In this temperature range the solid methane exists in a phase (called phase II) with partial orientation of the free rotors. We adapted an analytical model due to Ozaki .et .al. [1.2], which describes free and hindered rotor excitations in phase II valid for neutron energies below 6.5 meV, and convoluted it with a phonon model good for energies between 6.5 and 165 meV. The parameters of the model are consistent with neutron and Raman measurements of the excitations of phase II CH4. We present the double-differential cross section and total cross section and compare to the measurement of Grieger[3] and Whittemore[9].

1. Introduction

Cold neutrons are useful in studying the structure and dynamics of soft condensed matter and biological systems. Spallation neutron sources exist and are being constructed in the USA, UK, Europe, Japan, and China. LENS, the Low Energy Neutron Source under construction at the Indiana University Cyclotron Facility (IUCF), will be the first university based pulsed cold neutron facility in the US with a 3-fold mission of education, research, and cold neutron instrumentation development. [4].

High energy (~MeV) neutrons generated from a spallation target are moderated to cold neutron energies with hydrogenous materials like light water, liquid hydrogen and solid CH4 because hydrogen has a very large scattering cross section. The neutron scattering and slowing down properties of these materials, therefore, need to be studied to optimize neutron moderator design.

Solid methane moderators at spallation neutron sources are known to possess cold neutron source brightness greater than liquid hydrogen [5]. However the radiation damage and decomposition of the methane in high radiation environments have prevented their use in the highest power spallation sources. If this engineering problem can be solved (possibly through the use of recirculating systems of palletized methane in liquid helium or hydrogen)[6], it might be possible to operate solid methane moderators at temperatures well below 20K in solid phase II and increase the cold neutron brightness of high-power spallation sources. The low heat load on the LENS moderator due to the greatly reduced number and energy of fast neutrons and capture gammas will allow us to operate our solid methane moderator at temperatures well below 20K in the phase II region of the solid with infrequent warm-ups to release stored energy.

To our knowledge no model for the scattering law $S(Q,\omega)$ in phase II solid methane exists in the literature. We have therefore developed a model for $S(Q,\omega)$ for solid methane in phase II including rotational excitation in low temperature by adapting previous work of Ozaki [1].

2. The LENS Solid CH4 Cold Neutron Moderator

Solid methane at low temperature is the best known moderator material for cold neutron production for pulsed neutron sources. In addition to its high proton density (70% higher proton density than liquid hydrogen at 20K), methane also has a high density of low energy free rotational excitations even in the solid phase. This may explain why the observed neutron spectra from CH4 (see figure 1) possess the same temperature as the physical temperature of the medium in contrast to other moderators such as liquid hydrogen whose energy spectra correspond to an effective temperature that is about twice the physical temperature of the moderator [4, 7].

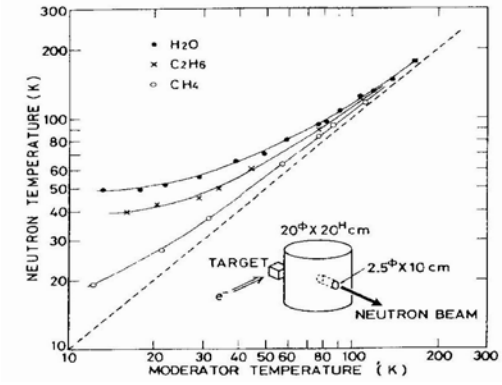

Figure 1: Effective neutron temperatures of thee moderator materials as a function of the moderator temperature

Methane moderators possess brightness 3~4 times that of liquid hydrogen around neutron energy 2meV for decoupled moderators as shown in figure 2.

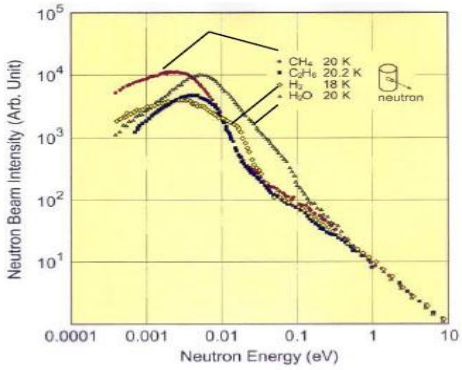

Figure 2: Neutron Beam Intensity and Neutron Energy of Moderator materials [7].

3. Theory of Solid Methane

In this section, we describe the rotational motion in phase II solid methane, measurement of the total neutron cross section up to 165meV and comparison with experimental data in 20K.

3.1 Phase II solid methane

Solid methane at low pressures has two distinct solid phases. At equilibrium vapor pressure, phase I appears from the triple point temperature (90.6K) to the transition temperature into phase II (20.49K).

In phase I, methane has a face-centered cubic structure with four orientationally disordered molecules per unit cell. This rotational motion of tetrahedral methane molecules remains slightly retarded even near the melting point of crystals.

In phase II, below 20.4K, center of mass of methane molecules is located on the site of the FCC lattice. But a structural transition to a partial orientational order occurs. This ordering of molecular orientation make methane has two different sublattices in phase II.

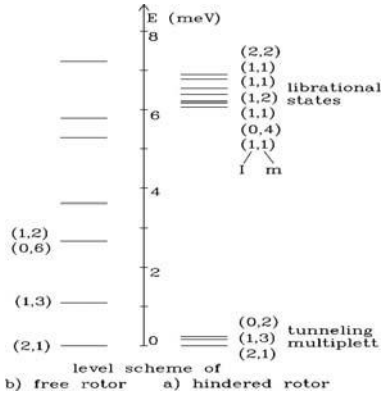

Figure 3: Rotational level scheme of methane in solid phase II.

Three-fourths of molecules are hindered rotors that librate in the minima of a strong orientational potential of D_{2d} symmetry. Tunneling between the minima of this potential produce a splitting of the ground state multiplet, which has energy levels at 0.0, 0.16, 0.24 meV (see figure 3). The librational states start at E_{lib} =6.5meV. The remaining 1/4 of the molecules rotate almost freely in a cubic crystalline field of symmetry O_h (see figure 4). The lowest levels are 0.0, 1.09 and 2.15 meV. These molecules are referred as free rotors [3].

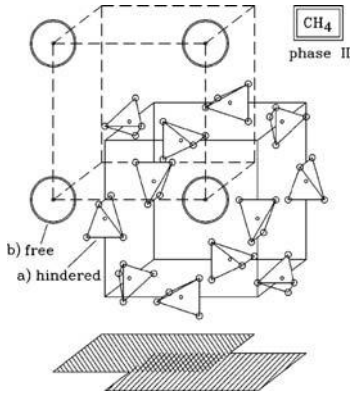

Figure 4: Structure of solid methane in phase II: of molecules are hindered rotor and are free rotor.

3.2 Total neutron cross section of the solid methane

We calculated the total neutron cross section in phase II as a function of incident energy E_i and temperature in the range $0.1meV < E_i < 165meV$ using the theoretical work of Ozaki [1]. The mechanism of the neutron scattering by the protons is calculated from the differential cross section in terms of the incident energy of neutron, momentum transfer and temperature. The double differential cross section is proportional to the scattering function $S(Q,\omega)$.

$$\frac{d^2\sigma}{d\Omega dE} = \frac{k_f}{k_i} b^2 S(Q,\omega) \qquad (3.2.1)$$

The dependence of the total cross section σ_{tot} on E_i may be divided into two energy regions in this calculation. In low energy region ($E_i < 6.5meV$), the behavior of protons is like bound particles and the cross section is dominated by the rotational states like hindered and free rotor states.

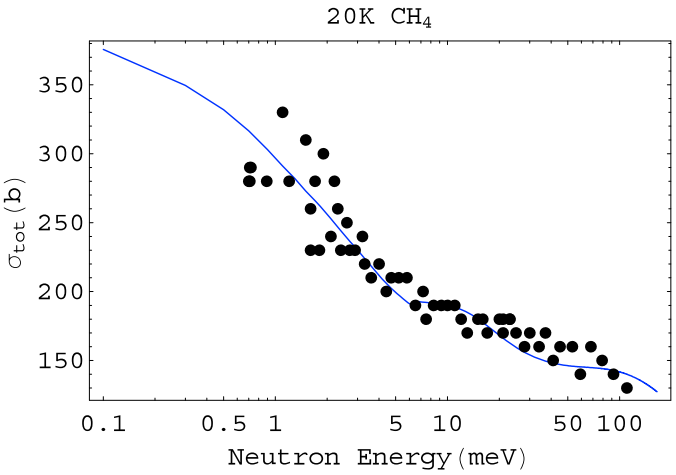

Figure 5: Neutron Total cross section of Solid Methane at 20K [5]

The scattering function in this region can be expressed as

$$S(Q,\omega) = Exp(-(\gamma_{trans} + \gamma_{vib})Q^2) \otimes (S^{el}_{rot}(Q)\delta(\omega) + S^{inel}_{rot}(Q,\omega)) \,. \tag{3.2.2}$$

The rotational scattering functions $S(Q,\omega)^{el}_{rot}$ and $S(Q,\omega)^{inel}_{rot}$ can be expressed as follows

$$S(Q,\omega)^{el}_{coh} = e^{-\gamma Q^2} \sum_{i,f} p_i(T) \frac{(b^2_{coh,C}\delta_{i,f} + 8 b_{coh,C} b_{coh,P} j_0(Qr) + 16 b_{coh,P} {j_0}^2(Qr))}{(b_{coh,C} + 4 b_{coh,P})^2}$$

$$S(Q,\omega)^{el}_{incoh} = e^{-\gamma Q^2} \sum_{i,f} p_i(T) \frac{3}{4} j_0^2(Qr) < I(I+1) >_T \tag{3.2.3}$$

and

$$S(Q,\omega)^{inel}_{coh} = e^{-\gamma Q^2} \sum_{i,f} p_i(T) \sum_{l=1}^{\infty} (2l+1) j_l^2(Qr) \overline{F}_l^{i,f} \delta(h\omega + E_i - E_f)$$

$$S(Q,\omega)^{inel}_{incoh} = e^{-\gamma Q^2} \sum_{i,f} p_i(T) \sum_{l=1}^{\infty} (2l+1) j_l^2(Qr) \overline{G}_l^{i,f} \delta(h\omega + E_i - E_f) \tag{3.2.4}$$

The coefficients $\overline{F}_l^{i,f}$ and $\overline{G}_l^{i,f}$ are transition integrals between initial and final state. The numerical values of these integrals for $l \le 8$ were published by Ozaki et al. [1].

The total cross section is the sum of elastic and inelastic contributions:

$$\sigma_{tot} = \sigma^0 + \sigma' \tag{3.2.5}$$

where

$$\sigma^0 = A + B < I(I+1) >_T$$

$$\sigma' = 4\pi \sum_{i,f} p_i(T) m_f \sum_{l=1}^{\infty} (2l+1) \left[b^2_{coh,p} \overline{F}_l^{i,f} + b^2_{inc,p} \overline{G}_l^{i,f} \right] J_l(k_0,k) \tag{3.2.6}$$

with

$$A = 4\pi\left[16 b_{coh,p}^2 J_0(k_0,k) + 8 b_{coh,p} b_{coh,C} J^{'}(k_0) + b_{coh,C} J^{''}(k_0)\right]$$

$$B = 4\pi \frac{4}{3} b_{inc,p}^2 J_0(k_0,k_0) \tag{3.2.7}$$

and

$$J^{'}(k_0) = \frac{1}{2(k_0 r)^2}\int_0^{2k_0 r} x j_0(x)\exp[-\gamma\left(\frac{x}{r}\right)^2]dx$$

$$J^{''}(k_0) = \frac{1}{2(k_0 r)^2}\int_0^{2k_0 r} x\exp[-\gamma\left(\frac{x}{r}\right)^2]dx$$

$$J_l(k_0,k) = \frac{1}{2(k_0 r)^2}\int_{|k_0-k|r}^{(k_0+k)r} x j_l^2\exp[-\gamma\left(\frac{x}{r}\right)^2]dx \tag{3.2.8}$$

Here m_f is the multiplicity of the final states and $J_l(k_i k_f)$ are the integrals of spherical Bessel function $j_l(x)$ and the Debye-Waller factor. The sum of the mean square amplitude of $\gamma = 2.15\times10^{-4} nm^2$ was founded from the experimental data [3]. The C-H bond length r is given as 1.093×10^{-8} [1]. The elastic scattering cross section σ^0 is responsible for the different temperature dependences of two rotational modes. On the other hand, σ' depends on the spin-rotational states as well as E_i and T. The Ozaki model, however, is valid only in the energy range $E_i < 6.5meV$ since it neglects phonon scattering. Ozaki et al introduced a simple Debye-Waller factor to take account of this neglected degree of freedom [3].

When E_i is greater than $6.5meV$ the scattering is characterized not only by rotational modes ($E_{vib}= E_{lib}$ =6.5meV) but also by excitation of phonons.

$$S(Q,\omega) = Exp(-\gamma_{vib}Q^2)\otimes S_{rot}(Q,\omega)\otimes\sum_{n=0}^{\infty} S_{trans}^n(Q,\omega) \tag{3.2.9}$$

The term $S_{trans}^n(Q,\omega)$ represents the multi-phonon excitation contribution

$$S(Q,\omega)_{phonon}^n = Exp[-2W(Q)]\left\{\frac{\hbar^2Q^2}{2M}\frac{Z(\omega)}{\omega} < 1+n(\omega) > + \frac{1}{\hbar\Delta}Exp[\omega/\Delta^2\gamma(0)]F(x,y)\right\},$$

$$x = \omega/\Delta, y = 2WExp[\frac{-1}{2\Delta^2\gamma(0)^2}],\ F(x,y) = \sum_{n=2}^{\infty}\frac{y^n}{n!}\exp(\frac{-x^2/2n}{\sqrt{2\pi n}}), \tag{3.2.10}$$

where the quantities $W(Q),\Delta$, and $\gamma(o)$ are calculated from the density of states $Z(\omega)$ in the usual way[8].

$$\gamma(0) = \frac{\hbar^2}{2M}\int_0^{\infty} d\omega\frac{Z(\omega)}{\omega}n(\omega),\ \varepsilon = \frac{3}{4}\int_0^{\infty} d\omega Z(\omega)\coth(\frac{h\omega\beta}{2}),$$

$$\Delta^2 = \frac{4\varepsilon}{3\hbar\gamma(0)} - \frac{1}{\gamma(0)^2}, 2W(Q) = \frac{\hbar Q^2}{4M}\int_0^{\infty} d\omega\frac{Z(\omega)}{\omega}\coth(\frac{\hbar\omega\beta}{2}) \tag{3.2.11}$$

Therefore the cross section due to phonon excitation becomes

$$\sigma = \frac{b_{inc,p}^2 2\pi}{k_i^2}\int_{|k_0-k|}^{|k_0+k|} QdQ\int_{-\infty}^{\infty} d\varepsilon S(Q,\omega)_{phonon}^n \quad . \tag{3.2.12}$$

This integration was calculated numerically for $1 \le n \le 5$.

When E_i is greater than $165meV$, the first vibrational excitation level appears. In this energy regime, the multiple inelastic scattering $S(Q,\omega) = S_{vib}^{inel}(Q,\omega) \otimes S_{rot}^{inel}(Q,\omega) \otimes \sum_{n=0}^{\infty} S_{trans}^{n}(Q,\omega)$ mainly contribute to the evaluation of cross section. The protons in this region move almost feely on the surface of a sphere and the rotational, translational motion of the center of molecule can be included in the free limit. We expect the mass tensor approximation [11] including vibrational excitation can describe the cross section in this high energy region with more reliable way and the inclusion of this approximation into our model is still in progress [3].

The experimental total cross section is shown in figure 5 and compared to our theoretical model of phase II solid methane in 20K with $0.1meV < E_i < 165meV$ [3,9]. The incident neutron energy is given on a logarithmic scale. The total cross section from these scattering functions agrees with experimental data in the low energy regime and also reliably fit up to $E_i < 165meV$.

4. Analytical Model for Neutron Scattering in Solid CH4

We developed a simple analytical model to illustrate the dependence of the neutron energy spectrum and the average neutron energy on the number of scattering events in the moderator. The real neutron distribution should approximately consist of a Maxwell-Boltzmann spectrum and a 1/E slowing-down spectrum. We assume that the incident neutrons have only Maxwell-Boltzmann distribution for simplicity and that the CH4 molecules are distributed evenly in the ground and first excited states before first scattering. During scattering process, neutrons diminish in energy from scattering with these molecules.

The procedure of each scattering simulation is as follows. First, the number of neutron N are distributed on Maxwellian flux curve at 300K as figure 6.

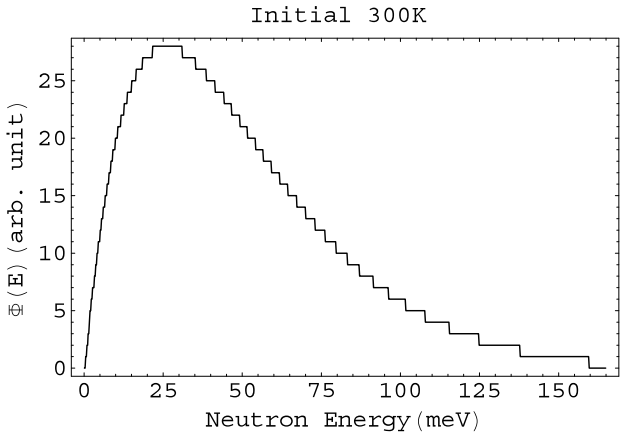

Figure 6: The Maxwell-Boltzmann Distribution of Neutron at 300K

The x axis in this plot is neutron energy (meV) and y axis is number of neutron in each 0.2 meV bin. The probabilities of the scattering cross section from ground and first excited state to higher energy states are calculated from our cross section model and absorption is included. Finally the neutron distribution function is computed and the distribution after each time of scattering is updated.

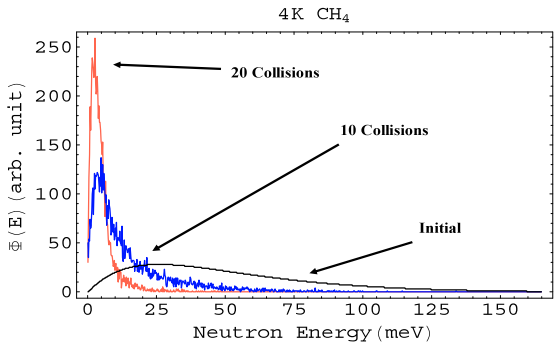

Figure 7: Evolution of the neutron energy distribution

Figure 7 shows the initial distribution and the simulation of neutron energy distribution after 10 (middle) and 20 (left) collisions. The relations of number of collisions N vs. average neutron energy <E> and the number of neutrons remaining after N collisions are plotted in figure 8. The left side of y axis scale for average energy and right side for the number of neutrons which survive after each bounce. The average energies and ratio of neutrons after bounces are 14.2 meV (84%) after 10 bounces and 4.97 meV (70%) after 20 bounces, respectively. The initial condition is 48.5 meV of average energy with 10000 neutrons. In this simulation, the number of neutron N after each collision is almost linearly decreased and the average energy diminish more rapidly. But after 25 time collisions, the average energy converges to a nonzero limit.

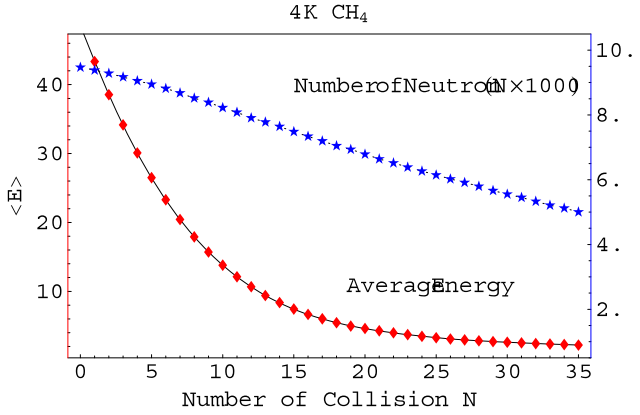

Figure 8: The relations numbers of collision vs. <E>and number of neutron

5. Experiment

A neutron energy distribution measurement was performed with the LENS target moderator reflector system at IUCF using a solid methane moderator held at a temperature of 4K using the neutron time of flight distribution. Constructed of 5N aluminum, the rectangular moderator vessel has 12 cm x 12 cm x 1cm dimension. The bottom surface is anchored on an aluminum rod which is attached to the heat exchanger. The detailed experiment procedure is described in the paper [10].

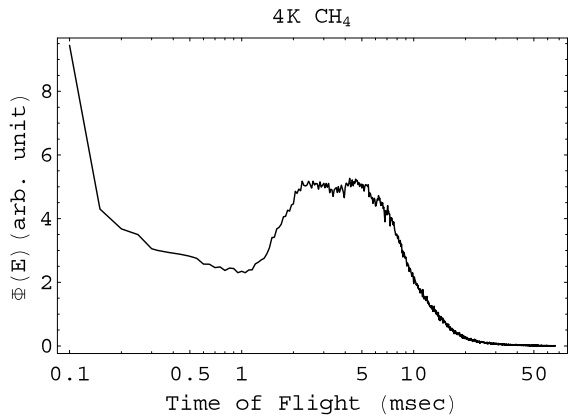

Figure 9: Neutron TOF spectrum from 4K solid methane

In figure 9, we show the measured time-of-flight spectra from the 4K solid methane. The black solid line in figure 10 shows experimental neutron energy distribution data obtained from time of flight measurement and blue line is our simulation after 18 collisions with probability matrix. The difference in high energy regime is due to epithermal distribution in experimental data which simulation didn't include for simplicity. But in low energy regime ($E_i < 10meV$), our scattering simulation shows comparatively good slowing-down effect which is due to the rotational modes in phase II solid methane.

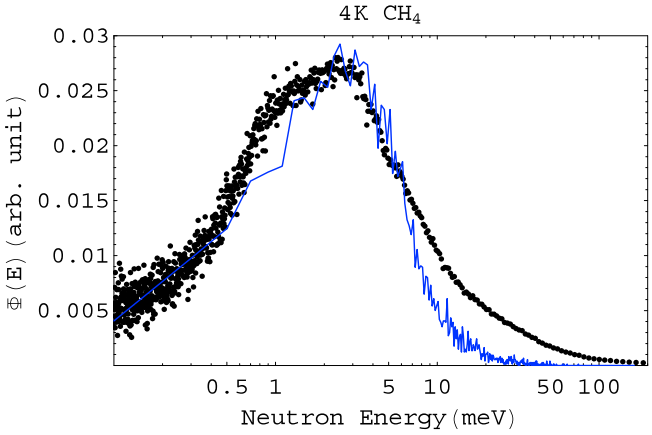

Figure 10: Neutron energy spectrum from 4K solid methane

6. Summary

A cross section model for cold neutron in solid methane was designed from the theoretical work of Ozaki [1] and compared with the experimental work of Grieger [3] and Whittemore [9] in 20K up to 165 meV incident neutron energy. Our theoretical model was built from a convolution of rotational and vibrational scattering functions S(Q,ω). This model showed good agreement with experimental data.

From this model, we could obtain reliable scattering functions which include rotational modes in low energy regime and phonon excitation in higher energy regime. We plan to implement our model in MCNP.

We also designed a simple analytical model to understand the relationships among the neutron energy spectrum, the number of collisions in the moderator, the remaining number of neutrons, and the average

neutron energy. Our simulation of neutron energy spectrum in 4K CH4 after 18 times collision compared well with the measured energy spectrum data from 4K solid CH4 moderator in LENS. Our simulation result show comparatively good agreement in the region $E_i < 10meV$.

Acknowledgements

This work has been supported by National Scientific Foundation (NSF) under project Number **NSF PHY-0242300, NSF PHY-0100348, NSF PHY-022056.**

References

[1] Y. Ozaki, Y. Kataoka, and T. Yamamoto, J. Chem. Phys. **73**, 3442 (1980).
[2] Y. Ozaki, Y. Kataoka, K. Otaka, and T. Yamamoto, Can. J. Phys. **59**, 275 (1981).
[3] S. Grieger, H. Friedrich, K. Guckelsberger, R. Scherm, and W. Press, J. Chem. Phys. **109**, 3161 (1988).
[4] D. V. Baxster, in *16th Meeting of the International Collaboration on Advanced Neutron Sources, Zeughaus, Germany, 2003*, edited by G.Mank and H. Conrad , p95.
[5] H.Conrad, in *16th Meeting of the International Collaboration on Advanced Neutron Sources, Zeughaus, Germany, 2003*, edited by G.Mank and H. Conrad , p921.
[6] J.M.Carpenter, in *16th Meeting of the International Collaboration on Advanced Neutron Sources, Zeughaus, Germany, 2003*, edited by G.Mank and H. Conrad , p39.
[7] K. Inoue, Y. Kitanagi, and H. Iwasa, Nucl. Inst. and Methods.**192**, 129 (1982).
[8] S.W. Lovesey, *Theory of Neutron Scattering from condensed matter* (Clarendon Press, Oxford, 1984), Vol. 1, p. 164
[9] W. L. Whittemore, A. W. McReynolds, General Atomic Report No. GA-2503, 1960 "Differential Neutron Thermalization" (unpublished).
[10] C. M. Lavelle, D. V. Baxter, M. B. Leuschner, M. A. Lone, W. Lozowski, H. Nann, N. Remmes, T. Rinckel1, Y. Shin, W. M. Snow, and P. E. Sokol1, "NEUTRONIC PERFORMANCE OF THE LENS TMR", *17th Meeting of the International Collaboration on Advanced Neutron Sources*, (to be published)
[11] R.G.Sachs, E, Teller, Phys. Rev. **60**, 18 (1941).